2023 International Conference on Optical MEMS and Nanophotonics (OMN) and SBFoton International Optics and Photonics Conference (SBFoton IOPC) | 979-8-3503-0402-2/23/$31.00 ©2023 IEEE | DOI: 10.1109/OMN/SBFOTONIOPC58971.2023.10230914

Ionization Model to Estimate the Density and Temperature of fs-Laser-Induced Plasmas in Air

Armando V. F. Zuffi
IPEN – CNEN
São Paulo, SP, Brazil
orcid.org/ 0000-0001-5705-1499

Jhonatha R. dos Santos
IPEN – CNEN
São Paulo, SP, Brazil
jhonatharicardo@gmail.com

Ricardo E. Samad
IPEN – CNEN
São Paulo, SP, Brazil
orcid.org/0000-0001-7762-8961

***Abstract*—We present a simple ionization model to assess the density of plasmas created in air by ionization induced by the electric field of ultrashort laser pulses. It calculates the average ionization induced by the laser taking into account the known threshold intensities for each ionic state, the beam spatial profile and the atmospheric composition, estimating the plasma density. The model density predictions are compared to experimental results obtained by a time-resolved Mach-Zehnder-like interferometer, and are also used as entry parameters to evaluate the plasma temperature by the Saha equation.**

Keywords — interferometry, plasma density measurements, laser-induced plasma

I. Introduction

The acceleration of electrons by lasers is a technique that has been gaining importance in recent years [1] due to its potential to decrease the size, complexity and cost of accelerators, favoring the diffusion of this technology to conventional laboratories, with the inevitable emergence of new science and applications [2]. Our research group has been working to implement the first laser-electron acceleration infrastructure in Brazil at the Nuclear and Energy Research Institute (IPEN) [3], and we are currently focusing efforts on different challenges ranging from the use of computational simulations [4, 5] to the manufacture and diagnosis of de Laval nozzles, gas jets, and laser-induced plasmas for [6, 7]. Within these accomplishments, we developed a time-resolved Mach–Zehnder-like interferometer (MZI) [6] to measure the temporal evolution of laser-induced plasmas with tens of femtoseconds temporal resolution, and we could determine the plasma density and temperature evolution since its creation by the laser pulse, up to 800 ps after it [6]. The measured plasma density integrated along the interferometer beam path was compared to a value estimated by a simple model, and a discrepancy of almost one order of magnitude was observed [6]. The model considered that air is composed by 80% N_2, which was ionized to the +5 state, and 20% O_2 ionized to the +4 state, and returned a higher density that the one measured.

Here we present a refinement of that model, considering the ionization dependence on the laser beam spatial intensity distribution, providing a more accurate estimate of the plasma electronic density, and a better assessment of the plasma temperature.

II. Methodology

This investigation used a Ti:Sapphire CPA laser system (Femtolasers Femtopower Compact Pro HR/HP) generating 25 fs (FWHM) ultrashort pulses, centered at 780 nm with 35 nm of bandwidth (FWHM), 200 µJ energy, at 4 kHz repetition rate in a laser beam with $M^2 \approx 1.2$. The pulses are sent into the pump-probe setup shown in Fig. 1, in which the probe beam is injected into a Mach-Zehnder interferometer that records transversal interferograms of the plasma created in air [6] by the pump pulses focused by a $f = 50$ mm off-axis parabolic mirror (OAP) to a $w_0 = 4$ µm beamwaist [6, 8].

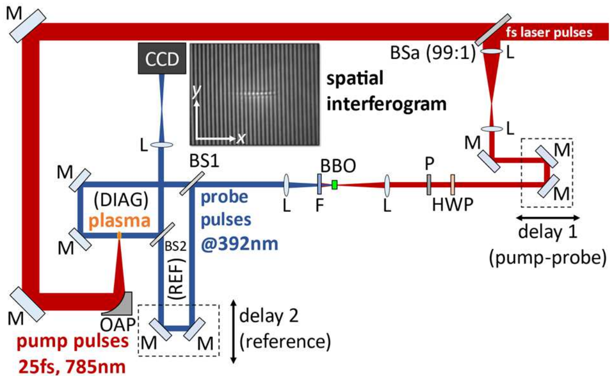

Fig. 1. Scheme of the pump-probe setup with the MZI.

The DIAG beam (Fig. 1) traverses the plasma, and accumulates a phase due to the optical path change created by the plasma, shifting the interferogram fringes; this integrated phase $\Delta\phi(x, y)$ can be obtained from the interferogram by Fourier transforms [6], and from it the plasma density distribution integrated along the DIAG beam path is given by:

$$n_e(x, y) = 4\pi^2 c^2 \varepsilon_0\, m_e/(e^2\lambda^2) \times \{1-[1+ \Delta\phi(x, y)\, \lambda/(2\pi l)]^2\}, \quad (1)$$

where e and m_e are the electron charge and mass, c is the speed of light, ε_0 is the vacuum permittivity, $\lambda = (392 \pm 2)$ nm is the probe wavelength, and $l = (20 \pm 2)$ µm is the $1/e^2$ diameter of the plasma. Using this procedure, the maximum plasma (electrons) density measured at the focus was $(3.2 \pm 0.4)\times10^{19}$ cm^{-3} [6].

By assuming the laser as a TEM_{00} Gaussian beam, the plasma is formed at the beamwaist by a 1.2×10^{16} W/cm^2 intensity (corresponding to 2.3×10^{16} W/cm^2 peak intensity). Considering the first five ionizations thresholds for nitrogen and oxygen given in Table I, the laser intensity is enough to dissociate and ionize both gases to the +4 state, and at the peak, nitrogen atoms are ionized to the +5 state. Taking the air atmospheric pressure density as $n_{air} = 2.5\times10^{19}$ cm^{-3} and the air composition into account, the estimated plasma density can be as high as 2.4×10^{20} cm^{-3} [6], 7.5 times higher than the measured density, indicating that the model used is not adequate.

To improve the estimated plasma density, we propose a model that uses the laser beam intensity radial profile and the gas species ionization intensities to calculate the spatial

This work was supported by FAPESP, SAE and CNPq grants.

distribution of the ionized electrons and average spatial density.

TABLE I. NITROGEN AND OXYGEN IONIZATION THRESHOLD INTENSITIES AND IONIZATION RADII

ionization state	Nitrogen		Oxygen	
	I_{th} (10^{16} W/cm²)	r_z (μm)	I_{th} (10^{16} W/cm²)	r_z (μm)
+1	0.018	6.23	0.014	6.39
+2	0.077	5.21	0.152	4.67
+3	0.225	4.29	0.405	3.74
+4	0.901	2.74	0.898	2.74
+5	1.469	1.85	2.693	-

The model can be understood by referring to Fig. 2, which shows the laser intensity profile at the focus ($w_0 = 4$ μm) and the radii at which the ionizations of oxygen (left half) and nitrogen (right half) occur, shown in Table I. This distribution considers the barrier suppression ionization, in which ionization only occurs once the intensity threshold is overcame [9].

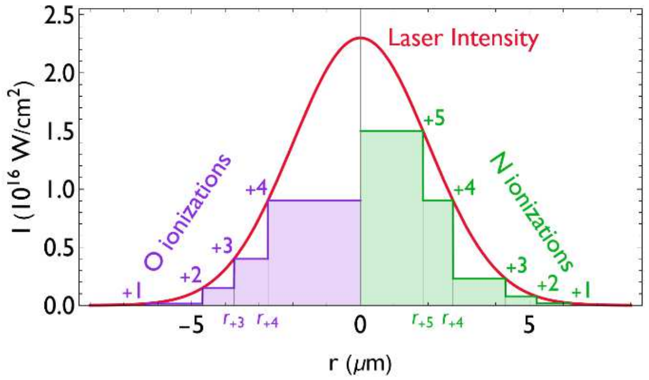

Fig. 2. Laser beam intensity profile at the focus, and spatial dependence of nitrogen and oxygen ionizations. The radial positions of only the two higher ionizations for each specias are indicated to avoid clutter.

Knowing the ionization radius r_z, where z is the ionization state of the atomic species, the average number of electrons released by that species, n_S, is given by:

$$n_S = 1/(2\, r_1) \sum 2\, z\, (r_z - r_{z+1}), \qquad (2)$$

where the summation index z runs from 1 (first ionization) to the maximum species ionization state reached, N_{max} (and $r_{N\max+1} = 0$). The plasma peak total electronic density will be:

$$n_e = 2\, n_{air} \times (0.8\, n_N + 0.2\, n_O), \qquad (3)$$

where n_N and n_O are the average number of released electrons for nitrogen and oxygen given by (2), respectively, and the factor 2 considers that there are 2 atoms per molecule.

III. RESULTS

The average number of released electrons for nitrogen and oxygen used in the model above are $n_N = 3.26$ and $n_O = 2.75$, resulting in a plasma density $n_e = 1.6\times10^{20}$ cm^{-3}, closer to the measure density, but still 5× above it. This discrepancy can be associated to processes that mitigate the laser intensity, such as plasma defocusing close to the focus [10] that impairs the ionization processes, reducing the plasma density. This could be corrected by a higher numerical aperture OAP.

The proposed model can be extended to calculate the atomic populations in each state, but in this case the area delimited by the ionization radii must be considered, multiplied by the ionization state. As an example, the ratio between the population of the two higher ionization states for the nitrogen atom (+5 and +4) is given by:

$$(n_{+5}/n_{+4}) = (5\,\pi\, r_{+5}^2)/\,[4\,\pi\,(r_{+5}^2 - r_{+4}^2)] = 1.05. \qquad (4)$$

This value can be used in the Saha equation to recalculate the plasma temperature temporal evolution presented in our previous work [6], providing the new results shown in Fig. 3. The observed ~25% increase in the plasma temperatures should be closer to the real values due to the more accurate population ratio provided by (4).

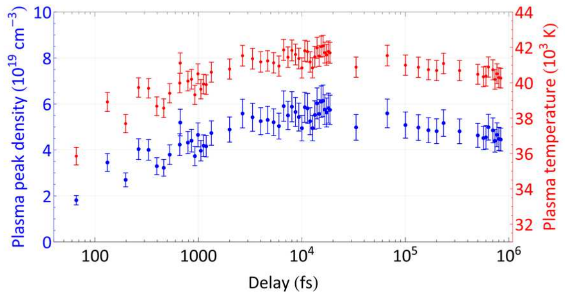

Fig. 3. Temporal evolution of the plasma density and estimated temperature using the presented ionization model.

IV. CONCLUSIONS

The presented model accounts for the ionization spatial distribution and allows better estimates of a laser induced plasma density and populations ratios, improving its characterization.

REFERENCES

[1] F. Albert, "2020 roadmap on plasma accelerators," New J. Phys., vol. 23, p. 031101, 2021.

[2] V. Malka, "Laser plasma accelerators," Phys. Plasmas, vol. 19, p. 055501, 2012.

[3] N. D. Vieira, "Laser wakefield electron accelerator: possible use for radioisotope production," 2021 SBFoton International Optics and Photonics Conference (SBFoton IOPC), São Carlos, SP, Brazil, 2021.

[4] E. P. Maldonado, R. E. Samad, A. V. F. Zuffi, J. R. d. Santos, and N. D. V. Jr., "Impact of He+N_2 concentration on self-modulated laser wakefield acceleration driven by pulses of a few TW," J. Opt. Soc. Am. B, vol. 40, pp. C141-C147, 2023.

[5] E. P. Maldonado, R. E. Samad, A. V. F. Zuffi, and N. D. V. Jr., "Simulation of self-modulated laser wakefield acceleration using few TW in the downramp injection and ionization injection regimes," Appl. Opt., vol. 62, pp. 3202-3207, 2023.

[6] A. V. F. Zuffi, J. R. d. Santos, E. P. Maldonado, N. D. V. Jr, and R. E. Samad, "Femtosecond Laser-Plasma Dynamics Study by a Time-Resolved Mach-Zehnder-Like Interferometer " Appl. Opt., vol. 62, pp. C128-C134, 2023.

[7] A. V. F. Zuffi, F. B. D. Tabacow, N. D. Vieira, and R. E. Samad, "Ultrafast laser micromachining of submillimetric de Laval nozzles in alumina for laser electron acceleration," 2022 SBFoton International Optics and Photonics Conference (SBFoton IOPC), 2022.

[8] R. E. Samad, A. V. F. Zuffi, E. P. Maldonado, and N. D. Vieira, "Development and Optical Characterization of Supersonic Gas Targets for High-Intensity Laser Plasma Studies," 2018 SBFoton International Optics and Photonics Conference (SBFoton IOPC), 2018.

[9] A. V. F. Zuffi, N. D. Vieira, and R. E. Samad, "Below-threshold-harmonics-generation limitation due to laser-induced ionization in noble gases," Phys. Rev. A, vol. 105, p. 023112, 2022.

[10] V. V. Semak, and M. N. Shneider, "Effect of power losses on self-focusing of high-intensity laser beam in gases," J. Phys. D Appl. Phys., vol. 46, 2013.